Conf-9011127--14

CONF-9011127--14

DE91 006631

Experiments Utilizing ICRF Heating on TFTR

J.R. Wilson, J.C. Hosea, M.G. Bell, M. Bitter, R. Boivin, E.D. Fredrickson, G.J. Greene, G.W. Hammett, K.W. Hill, D.J. Hoffman*, H. Hsuan, M. Hughes†, A.C. Janos, D.L. Jassby, F.C. Jobes, D.W. Johnson, C.K. Phillips, D.K. Mansfield, K.M. McGuire, S.S. Medley, D. Mueller, Y. Nagayama+, M. Ono, D.K. Owens, H.K. Park, M. Phillips†, A.T. Ramsey, G.L. Schmidt, S.D. Scott, J.E. Stevens, B.C. Stratton, E. Synakowski, G. Taylor, M. Ulrickson, K.L. Wong, M.C. Zarnstorff, S.J. Zweben

Princeton Plasma Physics Laboratory
Princeton, New Jersey 08543

*Oak Ridge National Laboratory
Oak Ridge, Tennessee 08731

†Grumman Corporation
Princeton, New Jersey 08540

+University of Tokyo
Tokyo, Japan

MASTER

ABSTRACT

A variety of experiments have been performed on the TFTR tokamak utilizing ICRF heating. Of special interest has been the insight into plasma performance gained by utilizing a different heating scheme other than the usual NBI. Utilizing ICRF heating

DISTRIBUTION OF THIS DOCUMENT IS UNLIMITED

allows control over the power deposition profile independent of the plasma fueling profile. In addition, by varying the minority concentration the power split between ion and electron heating can be varied. Confinement has been examined in high recycling gas fueled discharges, low recycling supershot plasmas, and peaked density pellet fueled discharges. Global confinement is found not to be affected by the method or localization of plasma heating, but the calculated local diffusivities vary with the power deposition profile to yield similar global values. In addition, sawtooth stabilization observed with ICRF heating has been investigated and found to occur in qualitative agreement with theory. ICRF sawtooth stabilized discharges exhibit peaked temperature and density profiles and have a safety factor q which appears to fall well below unity on axis.

DISCLAIMER

This report was prepared as an account of work sponsored by an agency of the United States Government. Neither the United States Government nor any agency thereof, nor any of their employees, makes any warranty, express or implied, or assumes any legal liability or responsibility for the accuracy, completeness, or usefulness of any information, apparatus, product, or process disclosed, or represents that its use would not infringe privately owned rights. Reference herein to any specific commercial product, process, or service by trade name, trademark, manufacturer, or otherwise does not necessarily constitute or imply its endorsement, recommendation, or favoring by the United States Government or any agency thereof. The views and opinions of authors expressed herein do not necessarily state or reflect those of the United States Government or any agency thereof.

I. INTRODUCTION

The ICRF experiments on TFTR[1,2,3] have been extended to a variety of plasma conditions. These include high recycling gas fueled discharges, NBI fueled supershot plasmas, and pellet fueled discharges.

The main emphasis of the ICRF program on TFTR is to support enhanced parameters in future D-T experiments. Although the ICRF system is envisioned to have significantly less power (ultimately 12.5 MW) than the NBI system (35 MW), the strong central electron heating by the rf power is still expected to raise the α production rate and β_α of the D-T plasmas on TFTR and thereby facilitate the α physics experiments. In addition, the ability to stabilize the sawtooth instability[4,5,6] could prove essential to achieving the best performance in the highest heating power, highest plasma current D-T experiments.

To prepare for these experiments, we have investigated the behavior of transport and confinement during ICRF heating and studied the conditions for sawtooth stabilization. These investigations will be discussed in the sections below.

II. TECHNICAL ASPECTS OF ICRF ON TFTR

ICRF heating is applied to TFTR utilizing two antennas mounted in adjacent midplane ports. Each antenna consists of two radiating elements separated toroidally, with independent phase control. For all of the experiments discussed here, the elements are phased 180° apart. Power is applied from four rf generators operating at 47 MHz. This frequency allows operation in the ^{3}He minority mode

III. TRANSPORT AND CONFINEMENT DURING ICRF

A. L-Mode Discharges

In high recycling gas fueled discharges on TFTR, ICRF heating has been applied in both the hydrogen minority (B_T = 3.4 T) and helium-3 minority (B_T = 5.2 T) heating modes. The global confinement of these discharges is well described by NBI L-mode scaling.[7] The scaling with plasma current and power are in general agreement with the Goldston formula. Deviation from this scaling (up to a factor of 1.5) are observed when a large fraction of the stored energy is present in the energetic minority ions, particularly at low plasma density and for hydrogen minority heating where up to 30% of the stored energy can be in the energetic minority ions. These ions exhibit better confinement than the bulk plasma essentially transferring all of their energy to the thermal ions and electrons before diffusing significantly.

Comparing ICRF and NBI in L-mode discharges allows a variation in heating profile, heating channel (electron vs ion), and fueling. Parameters for two discharges are listed in Table I. The discharges have the same plasma current, density, and size. The power deposition, temperature, and thermal confinement profiles are shown in Fig. 1. The electron temperature profiles are obtained via Thomson scattering and the ion temperature profiles via the charge exchange recombination technique. The ICRF power deposition is calculated using the code SHOOT[8] in conjunction with the 1-D transport code SNAP. The hydrogen minority concentration is

at full toroidal field (5.2 T) and H minority mode at reduced toroidal field (3.2 T). One of the antennas and two of the rf sources are capable of broad band operation but this feature has not been utilized to date. Because of the antenna geometry and antenna plasma coupling requirements, ICRF experiments are restricted for high power operation to plasmas of large major radius (R ~ 2.6 M, a ~ 0.96).

During the past year, operations have been extended to higher power, longer pulse, and over a wider range of plasma density than previously reported.[4] Power levels up to 6.3 MW for 1 sec and 5.0 MW for 2 sec have been achieved. One antenna has achieved operation at 5.0 MW and a power density of 10 MW/m^2 while the other antenna has achieved 1.7 MW and 5 MW/m^2 operation. Damage to the second antenna prevented its operation at higher power levels. This damage is being repaired during the present shutdown and operation to the design level of 7 MW total injected power should be achieved. All experiments were carried out in the so-called dipole phasing. Although having lower plasma coupling than monopole phasing by about a factor of 2, dipole phasing has no problem associated with plasma-antenna interaction.[2]

Operation has been extended to high density ($\overline{n_e} \sim 8 \times 10^{19}$ m^{-3}) utilizing pellet injection. Operation to higher density will be attempted during the next run period utilizing multiple pellet injection. Strong central heating is observed up to densities of 2.5×10^{20} m^{-3} in agreement with modelling, indicating no problems in wave propagation or absorption at these densities.

adjusted so that the SNAP predictions of stored energy and neutron production agree with the experimental values to better than 10%. The H minority ICRF heating leads to strong central electron heating. Eighty percent of the absorbed power is coupled to electrons and 20% to ions with all the power deposition inside of r/a ~ 0.35. The 100 keV deuterium NBI heated plasma yields a broader power deposition profile that is a mixture (~50:50) of ion and electron heating with the power deposition occurring out to r/a ~ 0.7. In spite of these differences, the global thermal confinement times of these discharges are nearly identical ($\tau_{Eth\ rf}$ = 185 ms, $\tau_{Eth\ NBI}$ =176 ms). Examination of the derived radial dependence of τ_{Eth} (Fig. 1c) utilizing the 1-D time independent transport code SNAP indicates that thermal confinement is strongly degraded in the center for the ICRF case and rises to the NBI level only at r $\geq$ 0.7 a. Further examination shows that the enhanced diffusivity (Fig. 1d) is mostly in the electron channel (χ_e), i.e., the channel being heated.

To compare the efficiency of heating through the electron or ion channel, hydrogen minority and helium-3 minority heating have been compared. In Table II, the parameters for two ICRF discharges are listed. Neither shot exhibited sawtooth oscillations. As in the above case, hydrogen minority heating is mainly through the electron channel while helium-3 minority heating, due to the stronger coupling of the helium-3 ions to the thermal ions, tends to introduce more energy through the ion channel. In addition, the helium case is

slightly off axis heating ($r \sim 0.12\,a$), leading to a less energetic tail due to the lower power density of the rf from the reduced focusing of the rf waves. This less energetic tail in conjunction with the stronger drag of ^3He on the bulk ions leads to an increase in the ion heating at the expense of electron heating. Again, the H minority case shows strong central electron heating (70% electron, 30% ion for $r/a \leq 0.3$) while the ^3He minority case shows broader heating ($r/a \leq 0.5$) that is predominantly through the ion channel (85% ion, 15% electron). Examination of the global parameters shows essentially identical global thermal confinement but enhanced total confinements in the hydrogen case due to the ~25% non-thermal hydrogen tail. Radial profiles of temperature, power deposition, and confinement properties as derived by SNAP are shown in Fig. 2. The temperature profiles for both types of discharges are peaked even for the off axis heating case. The diffusivities are enhanced for the channel being heated and the enhancement is localized where the heat is applied. In particular, the off axis heating case in conjunction with the peaked temperature profiles leads to the inferred small central diffusivity.

The L-mode data leads one to believe that L-mode confinement manifests itself as a global quantity independent of heating channel, method, or profile. Temperature profiles are observed to be "resilient" with a tendency to remain peaked. If heat loss is then attributed to local heat diffusion, the derived diffusivities are seen to increase where the power

density is high and for the species the power is deposited in, resulting in temperature profiles that are generally peaked in all cases.

B. Pellet Injection Experiments

The correlation of local heating and enhanced thermal diffusivity observed in L-mode is not found during pellet-fueled discharges with peaked density profiles. Figure 3 shows the combination of pellet injection followed by ^3He minority ICRF heating. For a period of 350 ms following the pellet injection, there is small central heat diffusion (~1.0 m^2/sec) even though the power deposition is peaked on axis. During this time, the density and pressure profiles are strongly peaked. The global confinement during this time is enhanced over L-mode (× 1.6) even though a large non-thermal population does not exist. As the density profile relaxes, the enhanced confinement disappears and reverts to a state similar to the gas fueled cases, where χ_e is larger (~2.5 m^2/sec) in the center of the discharge and the global confinement agrees with the L-mode scaling value.

The next step in this program will be to extend the experiments using multiple pellet injection during the ICRF pulse to sustain the peaked density profile and to increase the plasma central density. For plasmas fueled with a single pellet, central densities of up to 2.5×10^{20} m^{-3} have been achieved. Effective central electron reheat upon the application of ICRF heating is observed at all densities,

indicating strong rf absorption in the plasma center at even the highest densities. At present, the central density is limited by the size of the perturbation from a single pellet. Extrapolation of the parameters achieved to date with pellets and ICRF heating indicate that for $\tau_E \sim 0.22$ sec (present value) and $P_{rf} \sim 12.5$ MW (the maximum planned for TFTR), central temperatures of up to 10 keV will be obtained at central density of 1.5×10^{20} m^{-3}.

C. Supershots with ICRF Heating

The addition of ICRF heating to supershot plasmas is expected to be a major benefit to the alpha-physics stage of TFTR operation. The aim of applying ICRF heating to a supershot plasma is to raise the central electron temperature, thereby increasing the neutral beam and alpha slowing down time and hence the density and beta of the alpha particles in the discharge.

ICRF heating utilizing both hydrogen and helium-3 minorities has been applied to low recycling beam fueled discharges. In both instances, strong central electron heating has been observed with no reduction in the total global confinement time, which is enhanced above L-mode by a factor of ~2. The increased central electron temperature is accompanied by an increase in the beam stored energy. Figure 4 shows the central electron temperature evolution for a supershot with 23 MW of NBI heating and 5 MW of ^3He

minority ICRF heating compared to a shot without the added rf power.

The strongly centralized rf power deposition into the electrons is shown in Fig. 5. Even though the total rf power is only 20% of the NBI power, the power to electrons for $r/a \leq 0.25$ is dominated by the ICRF. This central deposition leads to the 20% increase in central electron temperature. SNAP analysis indicates that this increase in central temperature leads to a 15% increase in stored beam energy. Analogously in a D-T plasma, it would lead to a similar increase in central β_α. For these shots the increase in temperature did not lead to an increase in neutron level due to an increased influx of carbon from the limiters which depleted the central deuterium density. This decrease in deuterium accounts for the decrease in thermal stored energy and thermal confinement time for this discharge although global confinement was not affected until 3.9 sec.

Lower power shots which do not have the full supershot enhancement (due to inadequate beam fueling) do show the neutron enhancement in the absence of the carbon influx. Changes to the top and bottom limiters during the present TFTR shutdown are being made to allow high power operation of large plasma supershots with reduced carbon influx.

III. SAWTOOTH STABILIZATION EXPERIMENTS

Sawtooth stabilization may be of particular importance on TFTR in D-T operations. The best supershots do not have sawteeth,

but as the power and stored energy increase, the plasma current must be increased to avoid MHD instability.[9] As the current is increased, the sawteeth tend to reappear.

A. Stability of High Recycling Discharges

Initial sawtooth stabilization experiments were performed in the gas-fueled high recycling regime. Sawtooth stabilization is observed as in JET[6] for strong central heating that produces a large energetic ion population. Direct on-axis heating is the most effective for stabilizing the sawteeth. During the sawtooth stable period, the temperature and density profiles peak. Stabilized sawteeth have been observed for periods of more than 1 sec, limited by the rf pulse width. Figure 6 shows a typical sawtooth stabilized discharge. Simulation of this shot utilizing the time dependent code TRANSP[10] indicates that the central q value falls from ~1 to 0.6 during the stabilized period and that the inversion radius should increase by about 7 cm in rough agreement with the 10 cm growth observed. This increase in inversion radius from r_{inv} = 28.5 cm ~ a/q(a) to a larger value r_{inv} = 38.5 cm indicates a strong peaking of the current profile in agreement with the peaking of the temperature profile. This agreement gives confidence that q is well below unity on axis during the stabilized period.

Comparison with the theories of Coppi et al.[4] and White et al.[5] indicate qualitative agreement with these theories. Figure 7 shows four different sawtooth stabilized discharges at different plasma currents and densities. The normalized

growth rate $\hat{\gamma}_i = \gamma_i / \omega_d$ is calculated using the ARES stability code[11] while the normalized $\hat{\beta}_h = \beta_h \omega_A / \varepsilon \omega_d$ has been obtained by performing spatial integrals over the fast ion tail as estimated by the SNAP + rf code. γ_i is the growth rate of the ideal m=1 instability, ω_d is the drift frequency of the fast ions, ω_A is the Alfven frequency, β_h the beta of the fast ions inside the q=1 surface, and $\varepsilon = r_{q=1}/R$. Note that as n_e increases for a fixed current the discharge is calculated to be more unstable since the pressure is larger. Since the simulation of the time evolution of the q profile indicate that the inversion radius grows throughout the stabilized period, it is postulated that the termination of the sawtooth free period occurs when the normalized growth rate increases such that the discharge evolves vertically out of the stable region. Tailoring the rf deposition profile such that the inversion radius does not continue to increase with time may be required to achieve a true steady-state sawtooth stable discharge.

B. Stability of NBI Heated Discharges

Most ICRF plus NBI supershot plasmas are already sawtooth stable before applying the ICRF. By studying a counter dominated NBI heated discharge that exhibits sawteeth, ICRF stabilization of an NBI heated discharge has been demonstrated (Fig. 8).

During the sawtooth stabilization period, the neutron emission is seen to increase by ~40%. To achieve this

stabilization required an increase in the toroidal magnetic field to focus the ICRF heating power into the strongly Shafranov shifted center of the discharge. This required shift again demonstrates that direct on-axis heating is most efficacious for ICRF stabilization of sawteeth. The power threshold for this case was between 3.0 and 3.5 MW of ICRF for an NBI power of 7.5 MW.

V. CONCLUSION

The addition of ICRF heating has allowed a greater flexibility in studying plasma behavior on TFTR. Confinement studies indicate that while global thermal confinement is independent of heating method, profile, or channel, the derived local diffusivities are strongly modified with the local χ's, increasing in value where the power deposition is large and specifically for the channel in which the heat is introduced. An exception to this rule is observed in pellet fueled discharges. When the density peaking is very large, the local χ is suppressed even with strong central heating and the global confinement is enhanced over L-mode. The presence of fast particles allows global confinement in excess of L-mode but does not affect the underlying thermal confinement. The superthermal ion population has been found to stabilize the sawtooth instability in qualitative agreement with theory. ICRF heating of supershots has led to increases in central electron temperature and stored beam energy without degradation of supershot confinement properties. In a D-T plasma, this increase in central electron temperature will

lead to increased n_α and β_α thus allowing a wider range of α physics to be studied on TFTR.

ACKNOWLEDGMENTS

We thank the TFTR and ICRF technical staffs for their fine efforts and Drs. H. Furth, P. Rutherford, D. Meade, and R. Hawryluk for their support of the ICRF project. This work is supported by US Department of Energy Contract # DE-AC02-76-CHO-3073.

REFERENCES

1 WILSON, J.R., BELL, M.G., CAVALLO, A., COLESTOCK, P.L., DORLAND, W., GARDNER, W., GREENE, G.J., HAMMETT, G., HAWRYLUK, R., HENDEL, H., HOFFMAN, D., HOSEA, J.C., JAEHNIG, K., JOBES, F., KAITA, R., KIERAS-PHILLIPS, C., LYSOJVAN, A., MANSFIELD, D., MEDLEY, S., MUELLER, D., OWENS, K., SMITHE, D., STEVENS, J.E., SWAIN, D., TAIT, G., TAYLOR, G., ULRICKSON, M., WONG, K.L., ZWEBEN, S., AND THE TFTR GROUP, "ICRF Heating on the TFTR Tokamak for P_{rf} Up to 2.5 MW" (Proc. 12th Int. Conf. on Plasma Phys. and Controlled Nucl. Fusion Res. Nice, 1988) Vol. I (IAEA) Vienna (1989) 691.

2 STEVENS, J., COLESTOCK, P., HOFFMAN, D., HOSEA, J., PHILLIPS, C.K., WILSON, J.R., BEER, M., BELL, M., BOIVIN, R., BRETZ, N., BUSH, C., CAVALLO, A., FREDRICKSON, E., GREENE, G., HAMMETT, G., HILL, K., JANOS, A., JASSBY, D., JOBES, F., JOHNSON, D., KAITA, R., KILPATRICK, S.J., LEBLANC, B., MCGUIRE, K., MEDLEY, S., NAGAYAMA, Y., MUELLER, D., MANSFIELD, D., OWENS, K., PARK, H.,

RAMSEY, A., SCHIVELL, J., SCHMIDT, G., SYNAKOWSKI, E., STRACHAN, J., STRATTON, B., TAYLOR, G., VON GOELER, S., WONG, K.L., ZWEBEN, S., AND THE TFTR GROUP, "ICRF Heating Up to the 4.5 MW Level on TFTR (Proc. 17th Eur. Phys. Soc. Conf. on Controlled Fusion and Plasma Phys. Amsterdam, 1990) Vol. 14B, 1048.

3 HOSEA, J.C., BEER, M., BELL, M.G., BITTER, M., BOIVIN, R., BRETZ, N.L., BUSH, C.E., CAVALLO, A., CHU, T.K., COHEN, S.A., COLESTOCK, P.L., DYLLA, H.F., EFTHIMION, P.C., FREDRICKSON, E.D., GOLDSTON, R.J., GREENE, G.J., GREK, B., GRISHAM, L.R., HAMMETT, G.W., HAWRYLUK, R.J., HILL, K.W., HOFFMAN, D.J., HSUAN, H., HUGHES, M., HULSE, R.A., JANOS, A.C., JASSBY, D.L., JOBES, F.C., JOHNSON, D.W., KAITA, R., KIERAS-PHILLIPS, C., KILPATRICK, S.J., LAMARCHE, P.H., LEBLANC, B., MANOS, D.M., MANSFIELD, D.K., MAZZUCATO, E., MCGUIRE, K.M., MEADE, D.M., MEDLEY, S.S., MIKKELSEN, D.R., MOTLEY, R.W., MUELLER, D., NAGAYAMA, Y., ONO, M., OWENS, D.K., PARK, H.K., PHILLIPS, M., RAMSEY, A.T., REDI, M.H., ROQUEMORE, A.L., SCHILLING, G., SCHIVELL, J., SCHMIDT, G.L., SCOTT, S.D., STEVENS, J.E., STRACHAN, J., STRATTON, B.C., SYNAKOWSKI, E., TAYLOR, G., TIMBERLAKE, J.R., TOWNER, H.H., ULRICKSON, M., VON GOELER, S., WILSON, J.R., WONG, K.L., ZARNSTORFF, M.C., ZWEBEN, S.J., ICRF Heating in Several Regimes on TFTR" (Proc. 13th Int. Conf. on Plasma Phys. and Controlled Nucl. Fusion Rec. Washington, 1990, IAEA-CN-53/E-1-5).

4 COPPI, B., DETRAGIACHE, P., MIGLIVOLO, S., PEGORARO, F., PORCELLI, F., Phys. Rev. Lett. 63 (1989) 2733.

5 WHITE, R.B., BUSSAC, M.N., ROMANELLI, R., Phys. Rev. Lett. 62 (1989) 539.

6 CAMPBELL, D. J., START, D.F.H, WESSON, J.A., BARTLETT, D.V., BHATNAGAR, V.P., BURES, M., CORDEY, J.L., COTTRELL, G.A., DUPPEREX, D.A., EDWARDS, A.W., CHALKS, C.D., GORMETANO, C., GOWERS, C.W., GRANETZ, R.S., HAMNEN, J.M., HELLSTEN, T., JACQUINOT, J., LAZZARO, E., LOMAR, P.J., LOPES CARDOZZO, N., MANTICA, P., SNIPER, J.A., STORH, D., STOTT, P.E., THOMAS, P.R., THOMPSON, E., THOMSEN, K., TONETTI, G., Phys. Rev. Lett. 60 (1988) 2148.

7 GOLDSTON, R.J., Plasma Phys. 26 (1984) 87.

8 SMITHE, D.N., PHILLIPS, C.K., HAMMETT, G.W., and COLESTOCK, P.L. (Proc. 8th Top. Conf. on Radio-Frequency Power in Plasmas Irvine, 1989) 338.

9 MANICKAM, J., ARUNASALAM, V., BARNES, C.W., BELL, M.G., BITTER, M., BOSCH, H.-S., BRETZ, N.L., BUDNY, R., BUSH, C.E., CAVALLO, A., CHU, T.K., COHEN, S.A., COLESTOCK, P.L., DAVIS, S.L., DIMOCK, D.L., DYLLA, H.F., EFTHIMION, P.C., EHRHARDT, A.B., FONCK, R.J., FREDRICKSON, E.D., FURTH, H.P., GAMMEL, G., GOLDSTON, R.J., GREENE, G.J., GREK, B., GRISHAM, L.R., HAMMETT, G.W., HAWRYLUK, R.J., HENDEL, H.W., HILL, K.W., HINNOV, E., HOSEA, J.C., HOWELL, R.B., HSUAN, H., HULSE, R.A., JAEHNIG, K.P., JANOS, A.C., DASSBY, D.L., JOBES, F.C., JOHNSON, D.W., JOHNSON, J.L., JOHNSON, L.C., KAITA, R., KIERAS-PHILLIPS, C., KILPATRICK, S.J., KRUPIN, V.A., KUO-PETRAVIC, G., LAMARCHE, P.H., LANGER, W.D., LEBLANC, B., LITTLE, R., LYSOJVAN, A.I., MANOS, D.M., MANSFIELD, D.K., MAZZUCATO, E., MCCANN, R.T., MCCARTHY, M.P., MCCUNE, D.C., MCGUIRE, K.M., MCNEILL, D.H., MEADE, D.M., MEDLEY, S.S., MIKKELSEN, D.R., MILLER, A., MONTICELLO, D.A., MOTLEY, R.W.,

MUELLER, D., MURAKAMI, Y., MURPHY, J.A., NIESCHMIDT, E.B., OWENS, D.K., PARK, H.K., PARK, W., RAMSEY, A.T., REDI, M.H., ROQUEMORE, A.L., RUTHERFORD, P.H., SAITO, T., SAUTHOFF, N.R., SCHILLING, G., SCHIVELL, J., SCHMIDT, G.L., SCOTT, S.D., SINNIS, J.C., STEVENS, J.E., STODIEK, W., STRATTON, B.C , TAIT, G.D., TAYLOR, G., TIMBERLAKE, J.R., TOWNER, H.H., ULRICKSON, M., VON GOELER, S., WIELAND, R.M., WILLIAMS, M.D., WILSON, J.R., WONG, K.L., YOSHIKAWA, S., YOUNG, K.M., ZARNSTORFF, M.C., ZWEBEN, S.J., "Stability of TFTR Plasmas (Proc. 12th Int. Conf. on Plasma Phys. and Controlled Nucl. Fusion Res. Nice, 1988) Vol. I (IAEA) Vienna (1989) 395.

10 HAWRYLUK, R.J., Coppi, B. editor Physics of Plasmas Close to Thermonuclear Conditions, Vol. I, 19, CSC, Brussels 1980.

11 HUGHES, M. and PHILLIPS, M. (Proc. 13th Int. Conf. on Plasma Phys. and Controlled Nucl. Fusion Res. Washington, 1990) IAEA-CN-53/D-2-8.

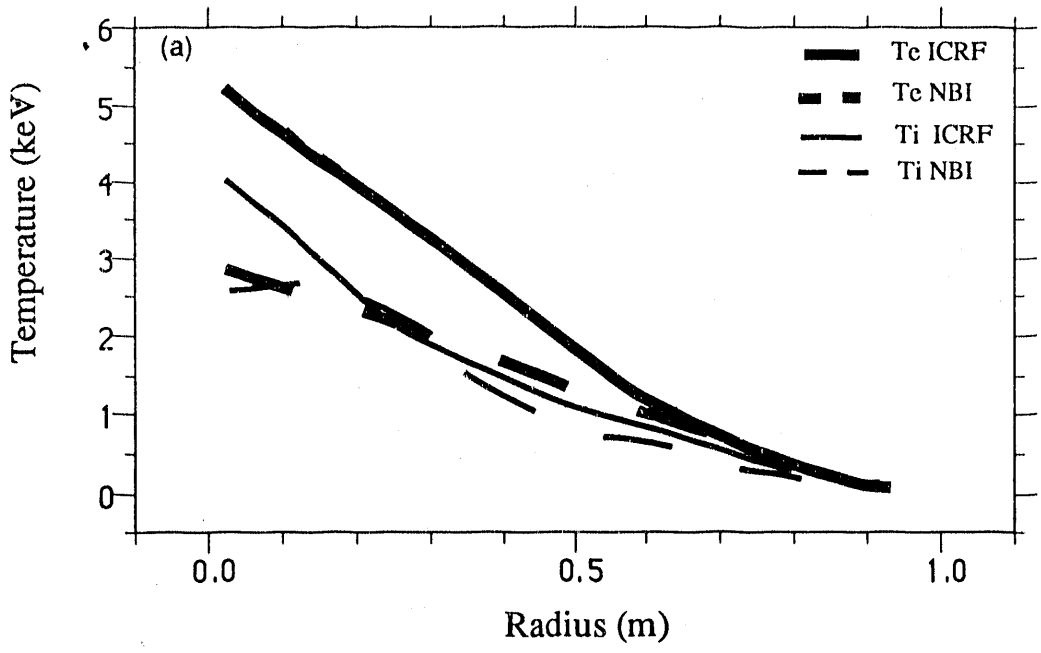
(a)
Tc ICRF
Tc NBI
Ti ICRF
Ti NBI
Temperature (keV)
0
1
2
3
4
5
6
0.0
0.5
1.0
Radius (m)

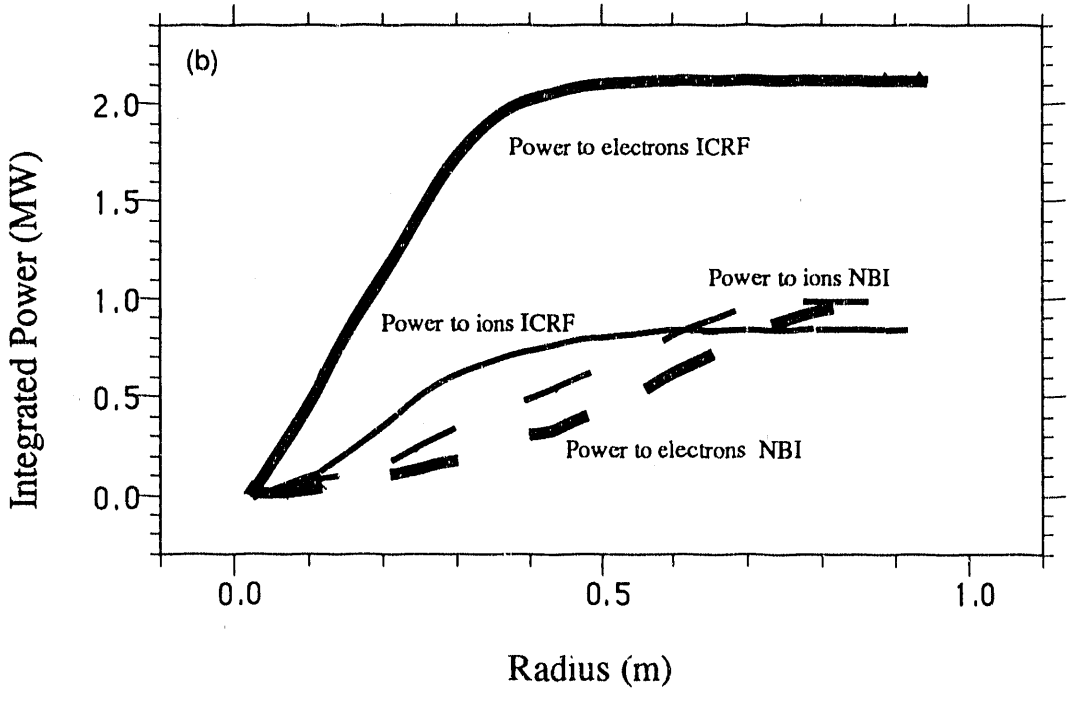
(b)
Power to electrons ICRF
Power to ions NBI
Power to ions ICRF
Power to electrons NBI
Integrated Power (MW)
0.0
0.5
1.0
1.5
2.0
0.0
0.5
1.0
Radius (m)

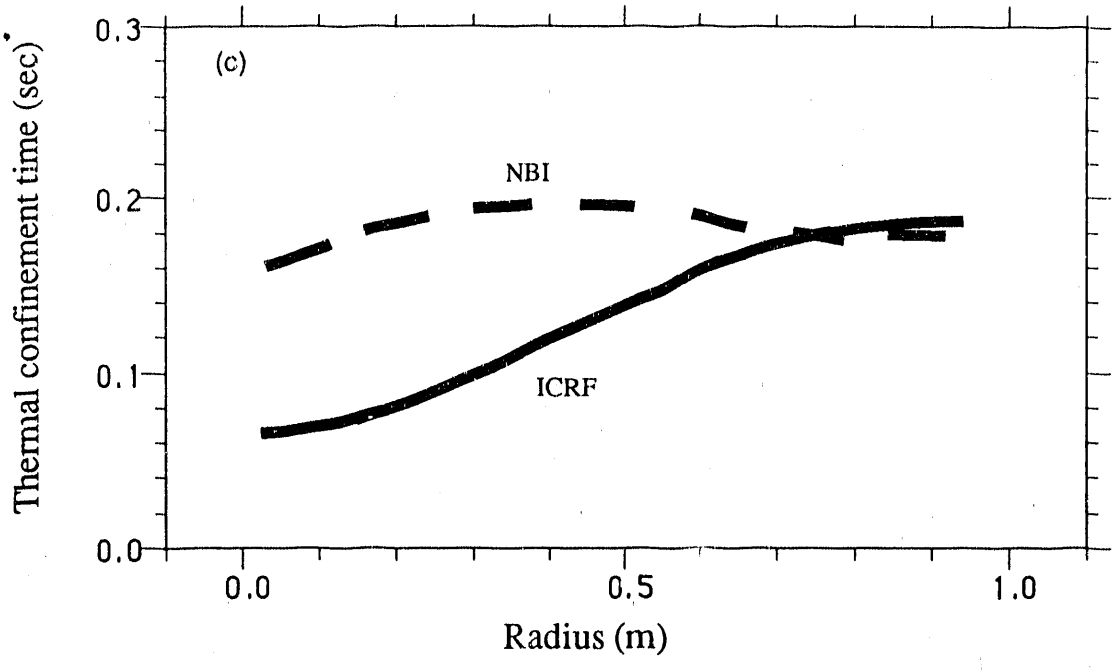
(c)
Thermal confinement time (sec)
0.3
0.2
0.1
0.0
NBI
ICRF
0.0
0.5
1.0
Radius (m)

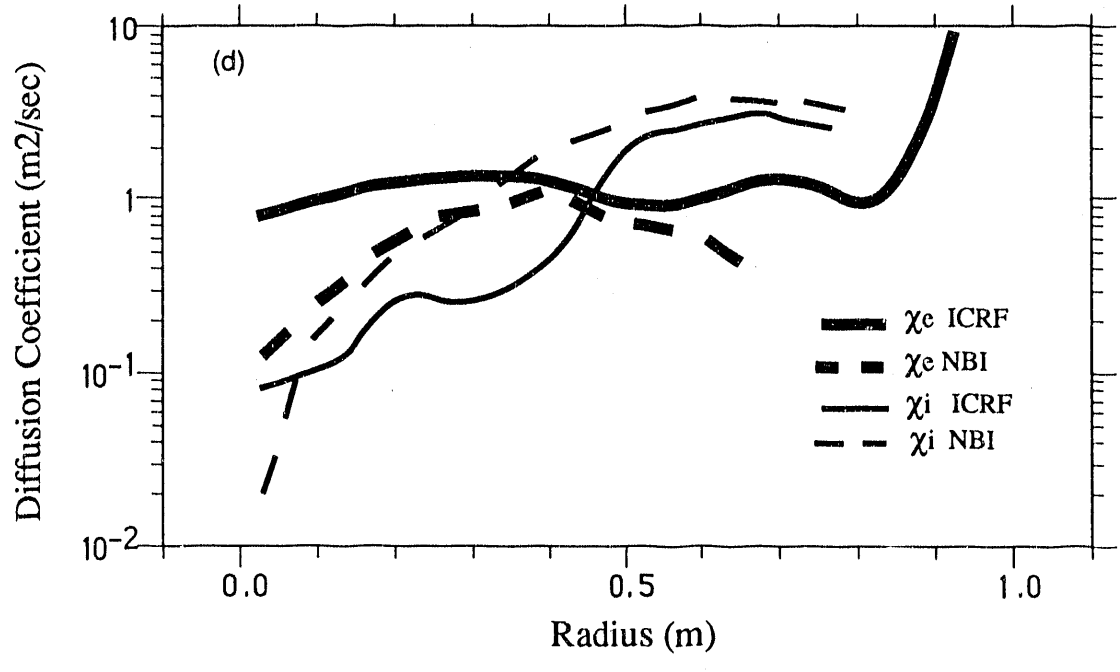
(d)
Diffusion Coefficient (m2/sec)
10
1
10-1
10-2
χe ICRF
χe NBI
χi ICRF
χi NBI
0.0
0.5
1.0
Radius (m)

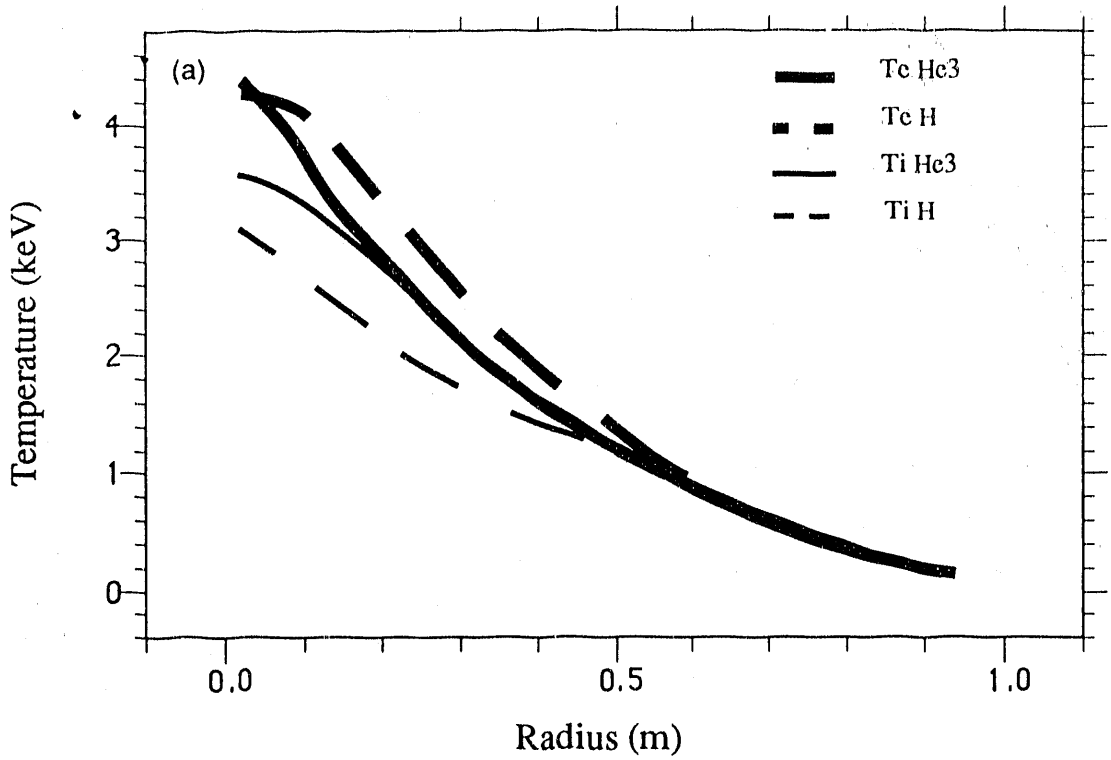
(a)
Tc He3
Tc H
Ti He3
Ti H
Temperature (keV)
0
1
2
3
4
0.0
0.5
1.0
Radius (m)

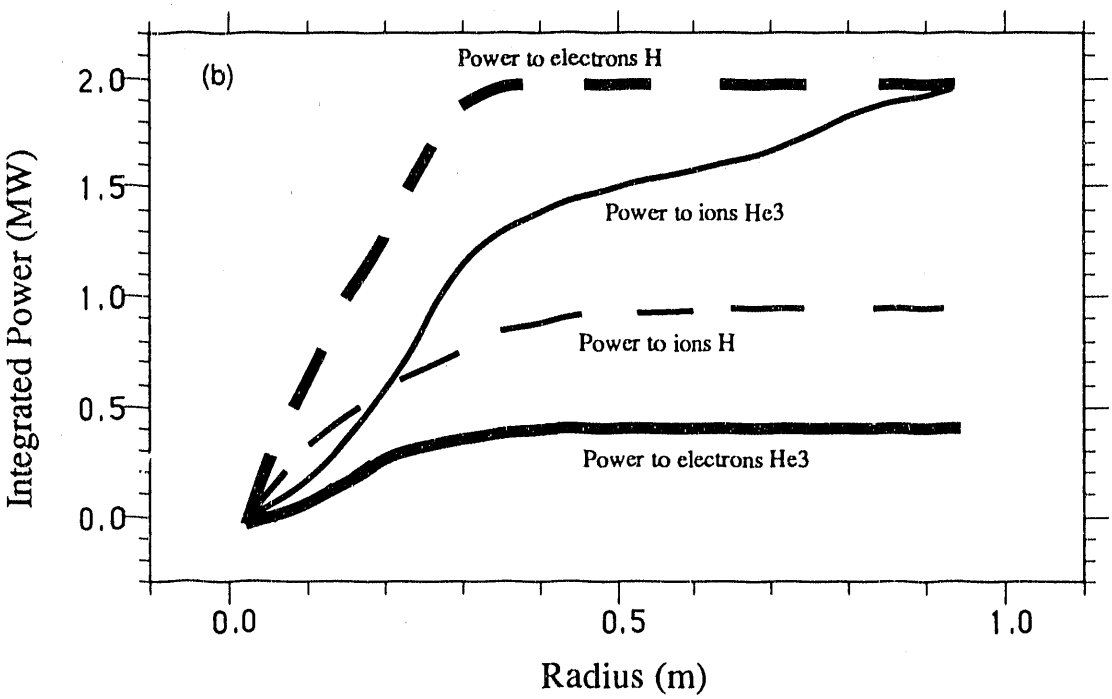
(b)
Power to electrons H
Power to ions He3
Power to ions H
Power to electrons He3
Integrated Power (MW)
0.0
0.5
1.0
1.5
2.0
0.0
0.5
1.0
Radius (m)

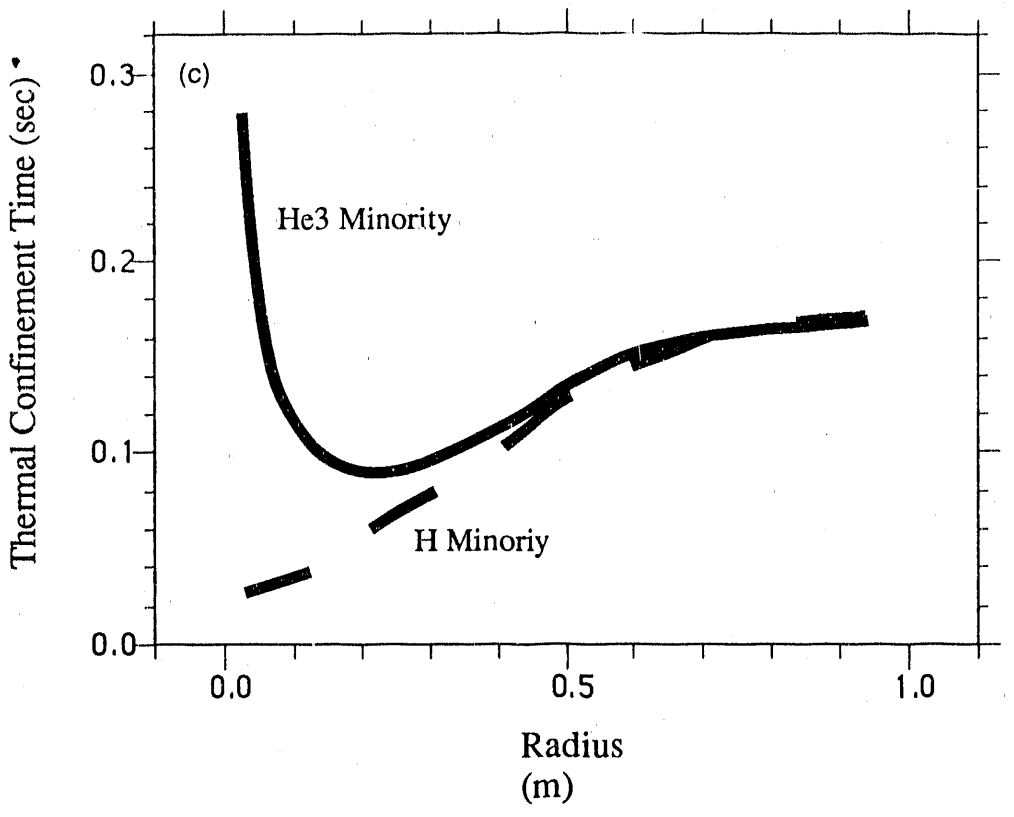
(c)
Thermal Confinement Time (sec)
0.3
0.2
0.1
0.0
He3 Minority
H Minoriy
0.0
0.5
1.0
Radius
(m)

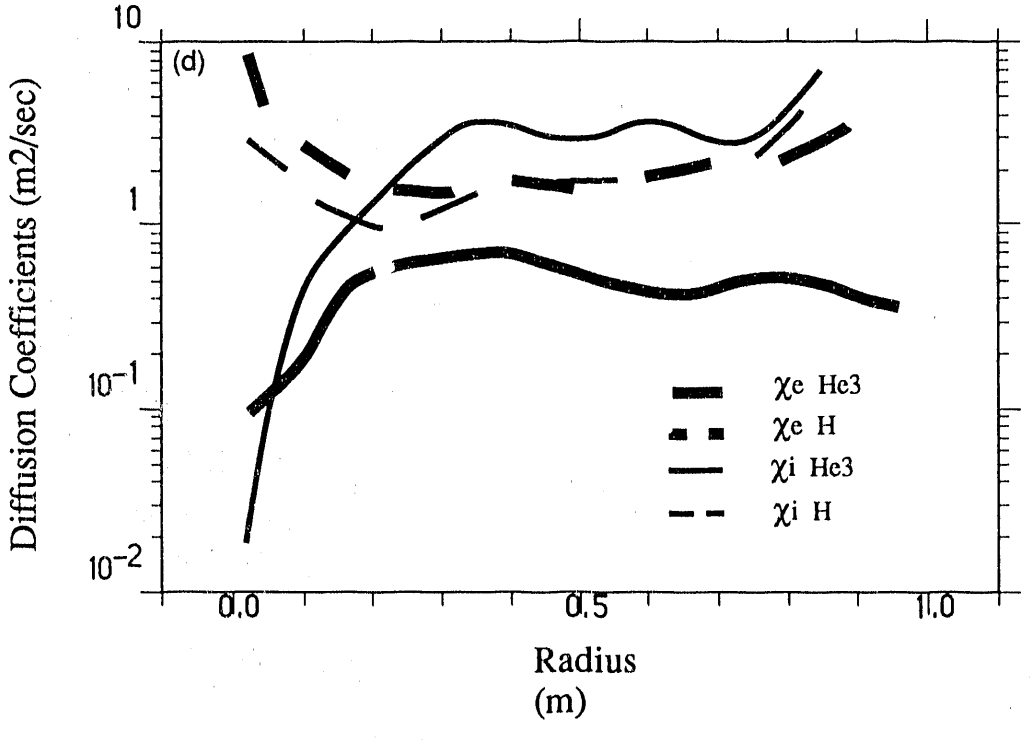
(d)
Diffusion Coefficients (m2/sec)
10
1
10^{-1}
10^{-2}
χe He3
χe H
χi He3
χi H
0.0
0.5
1.0
Radius
(m)

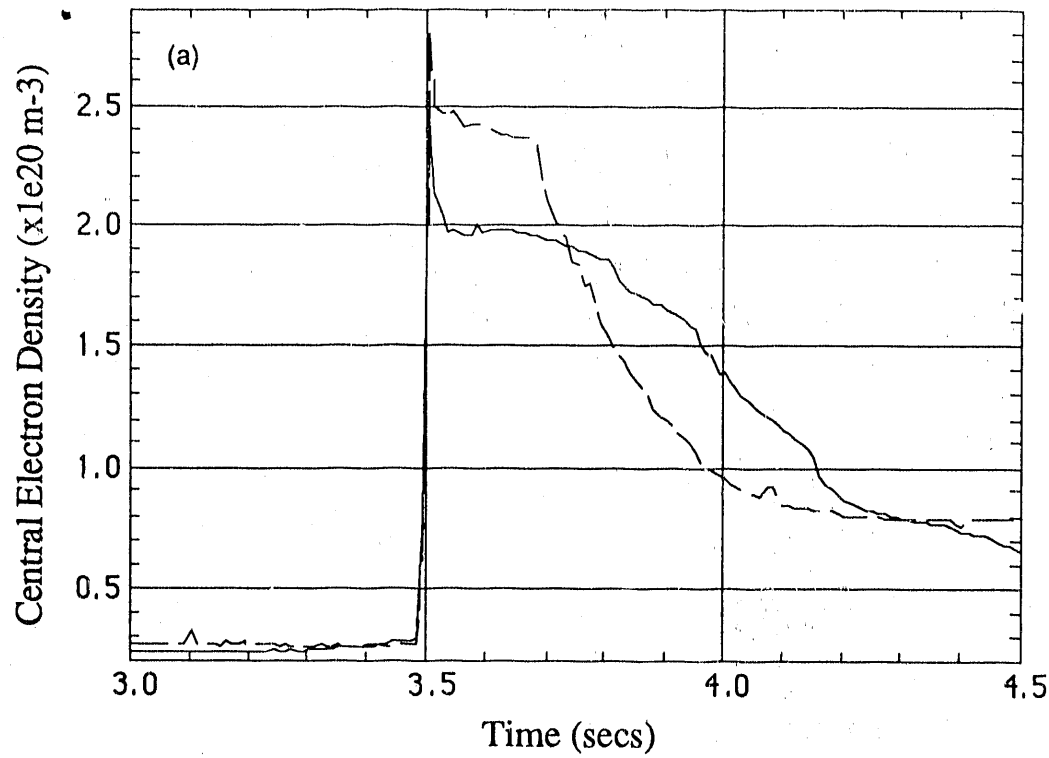
(a)
Central Electron Density (x1e20 m-3)
2.5
2.0
1.5
1.0
0.5
3.0
3.5
4.0
4.5
Time (secs)

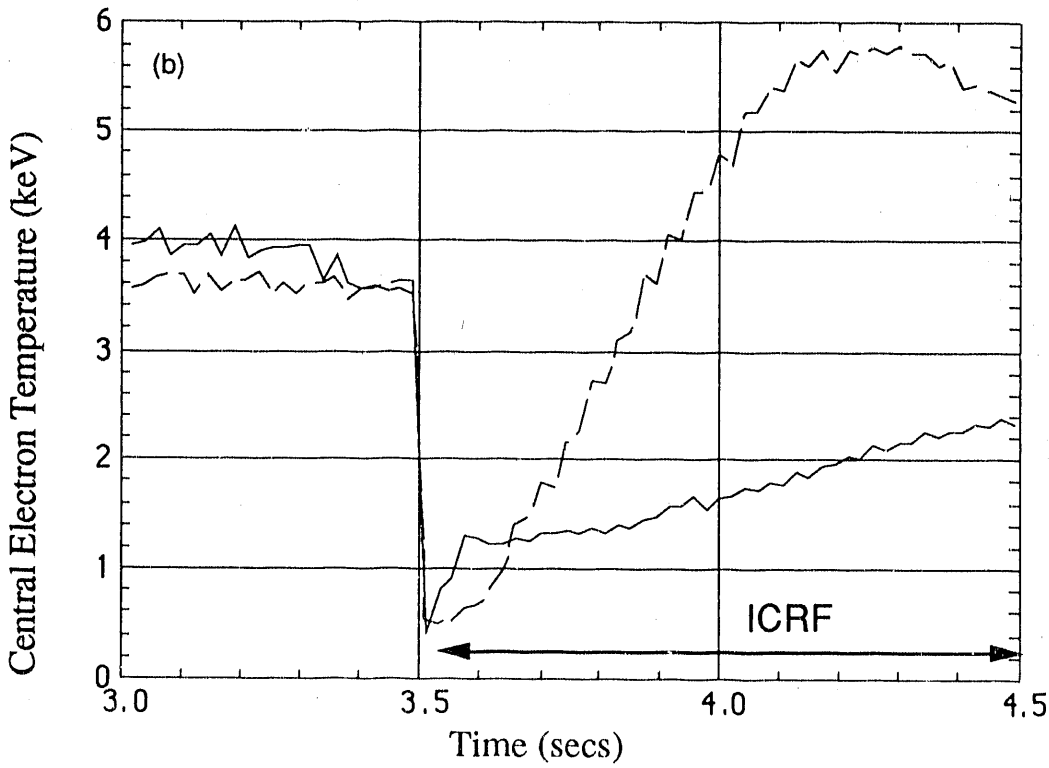
(b)
Central Electron Temperature (keV)
6
5
4
3
2
1
0
ICRF
3.0
3.5
4.0
4.5
Time (secs)

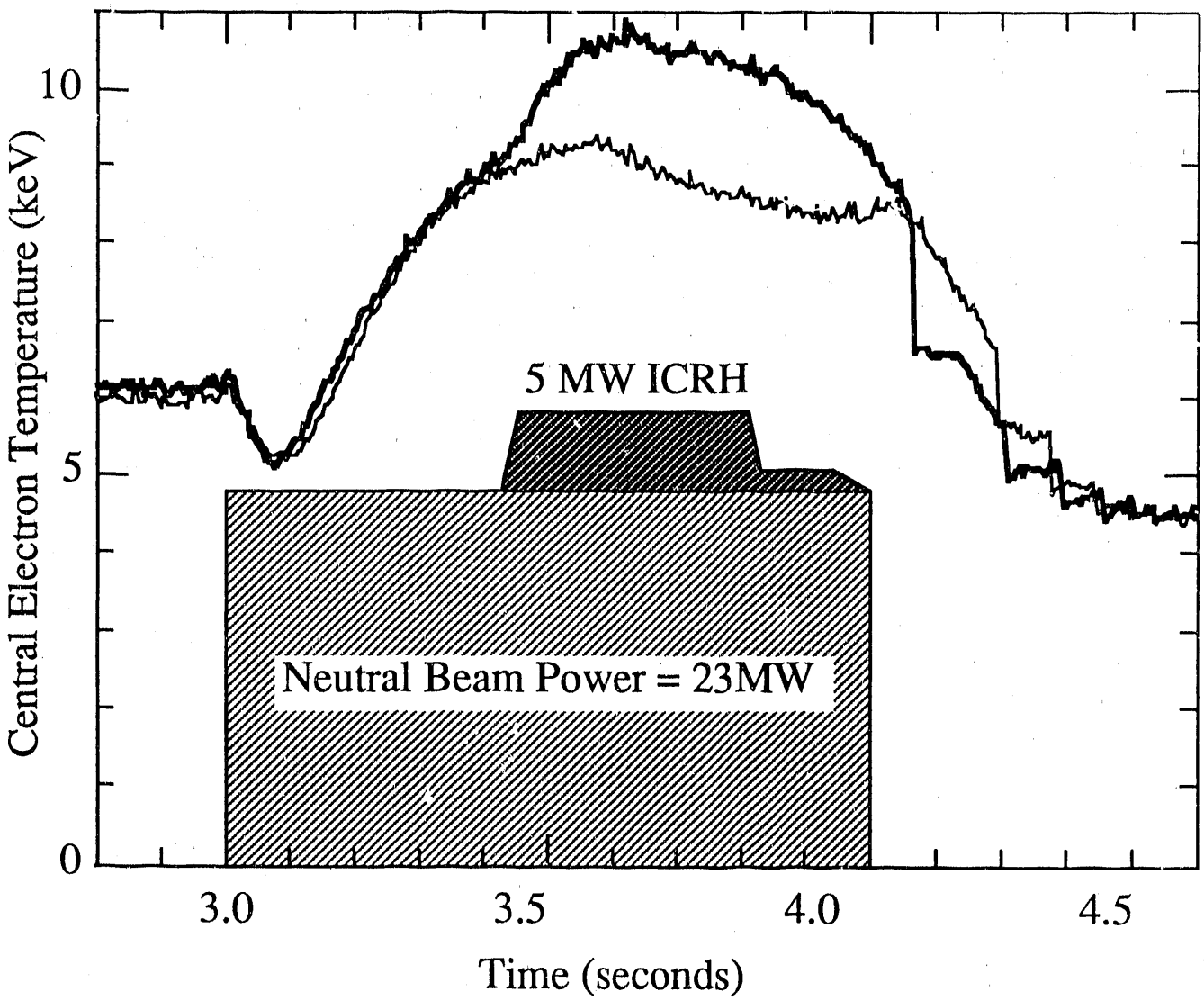
10
5
0
Central Electron Temperature (keV)
5 MW ICRH
Neutral Beam Power = 23MW
3.0
3.5
4.0
4.5
Time (seconds)

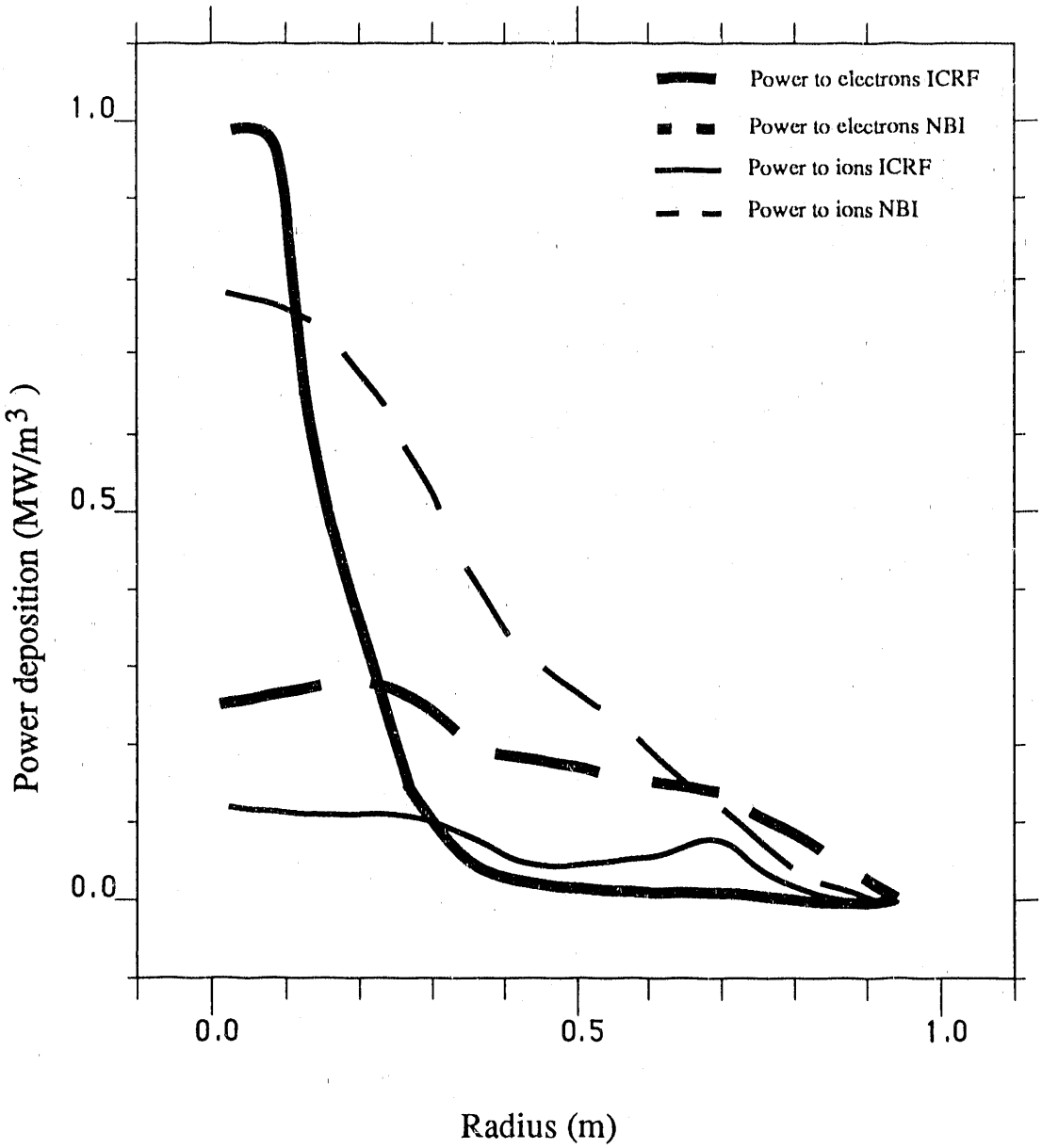
Power to electrons ICRF
Power to electrons NBI
Power to ions ICRF
Power to ions NBI
1.0
0.5
0.0
0.0
0.5
1.0
Power deposition (MW/m^3)
Radius (m)

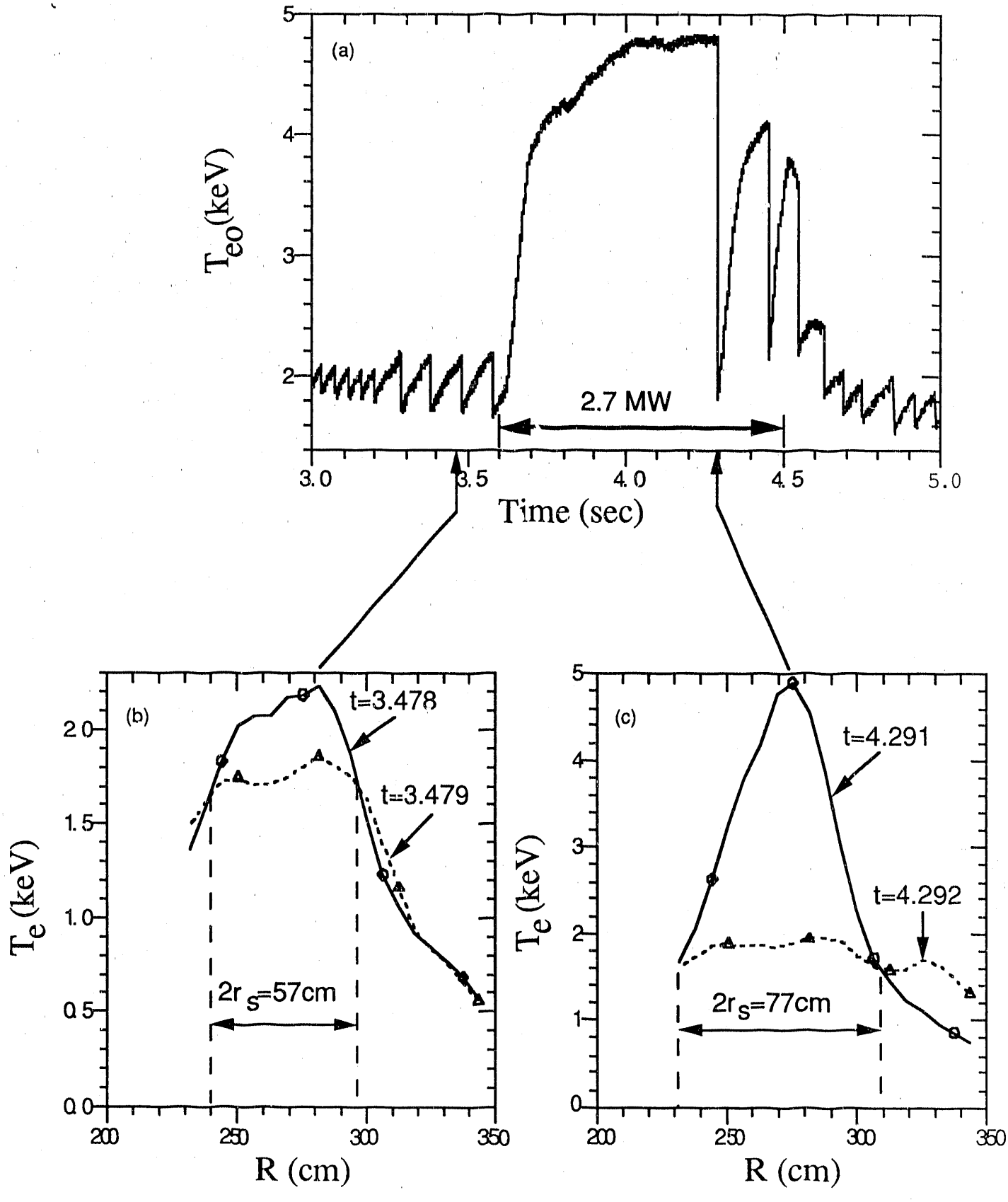
(a)
T_{eo}(keV)
2.7 MW
Time (sec)
(b)
t=3.478
t=3.479
$2r_s$=57cm
T_e (keV)
R (cm)
(c)
t=4.291
t=4.292
$2r_s$=77cm
T_e (keV)
R (cm)

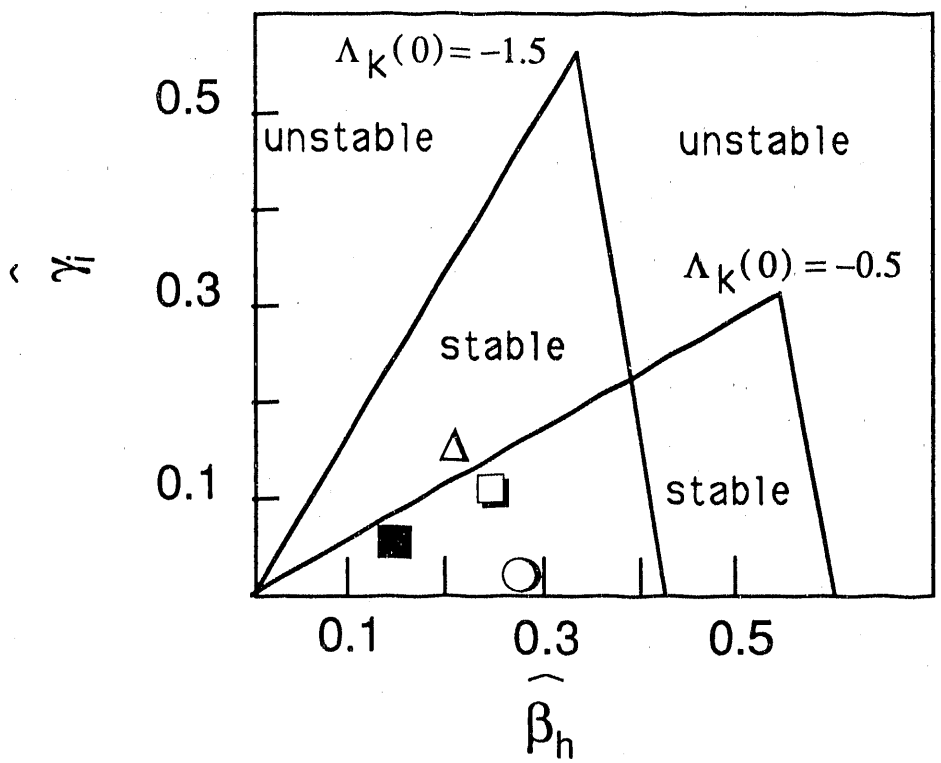
$\Lambda_K(0) = -1.5$
$\Lambda_K(0) = -0.5$
unstable
unstable
stable
stable
0.5
0.3
0.1
0.1
0.3
0.5
γ_i
$\hat{\beta}_h$

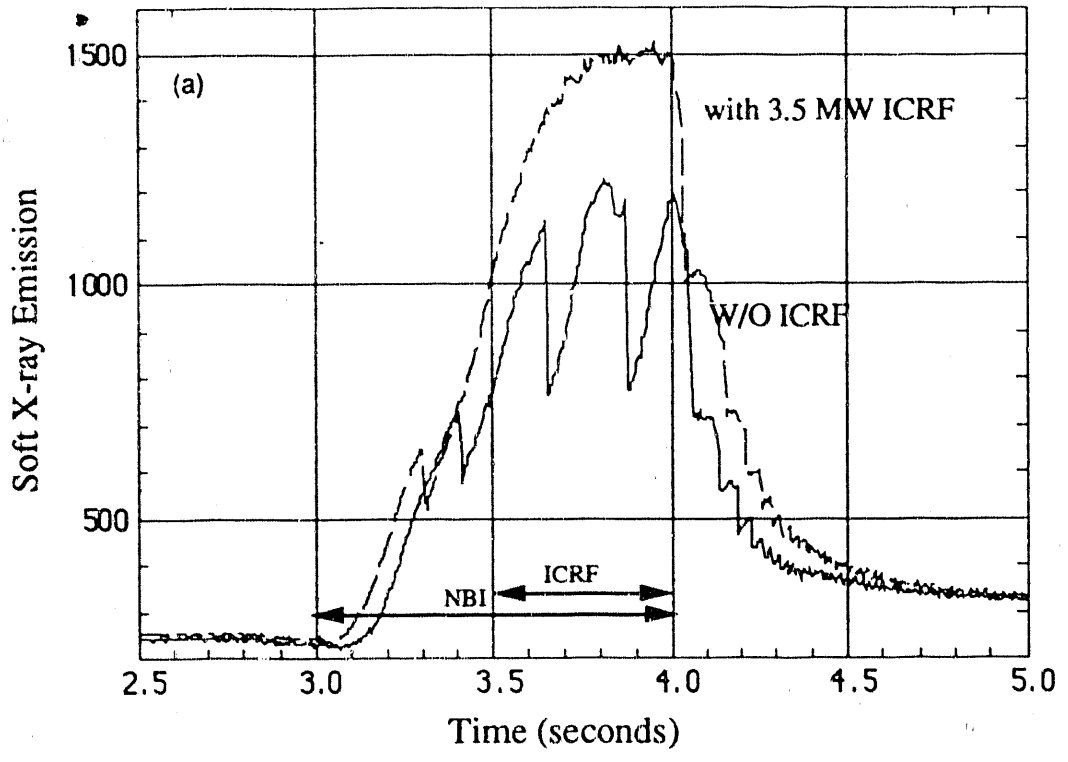
(a)
with 3.5 MW ICRF
W/O ICRF
ICRF
NBI
Soft X-ray Emission
1500
1000
500
2.5
3.0
3.5
4.0
4.5
5.0
Time (seconds)

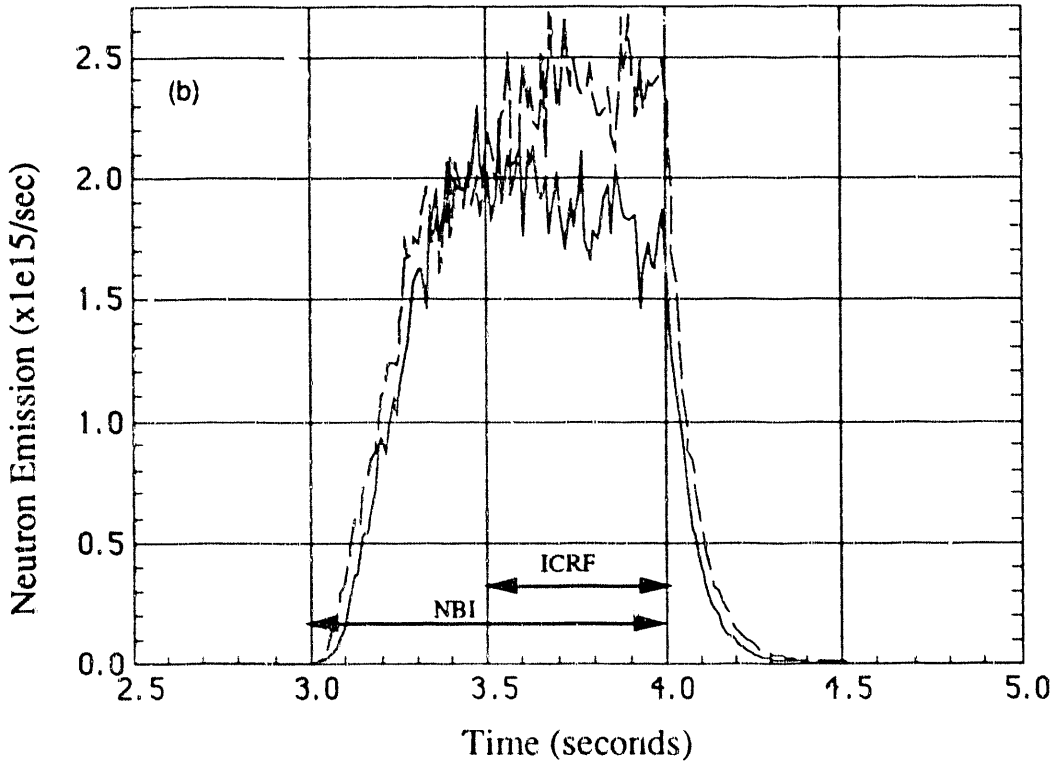
(b)
ICRF
NBI
Neutron Emission (x1e15/sec)
2.5
2.0
1.5
1.0
0.5
0.0
2.5
3.0
3.5
4.0
4.5
5.0
Time (seconds)

END

DATE FILMED

02 / 06 / 91